J|A|C|S

Article

Activation and Deactivation of a Robust Immobilized Cp*Ir-Transfer Hydrogenation Catalyst: A Multielement *in Situ* X-ray Absorption Spectroscopy Study

Grant J. Sherborne,[†] Michael R. Chapman,[†] A. John Blacker,[†] Richard A. Bourne,[†] Thomas W. Chamberlain,[‡] Benjamin D. Crossley,[§] Stephanie J. Lucas,[†] Patrick C. McGowan,[†] Mark A. Newton,[⊥,#] Thomas E. O Screen,[§] Paul Thompson,[⊥,#] Charlotte E. Willans,[†] and Bao N. Nguyen*,[†]

[†]Institute of Process Research & Development, School of Chemistry, University of Leeds, Woodhouse Lane, Leeds LS2 9JT, United Kingdom

[‡]School of Chemistry, University of Nottingham, Nottingham NG7 2RD, United Kingdom

[§]Yorkshire Process Technology Ltd., Leeds Innovation Centre, 103 Clarendon Road, Leeds, LS2 9DF, United Kingdom

[⊥]Department of Physics, University of Liverpool, Liverpool L69 7ZE, United Kingdom

[#]XMaS CRG, European Synchrotron Radiation Facility, 38043 Cedex, Grenoble, France

Ⓢ *Supporting Information*

ABSTRACT: A highly robust immobilized $[Cp*IrCl_2]_2$ precatalyst on Wang resin for transfer hydrogenation, which can be recycled up to 30 times, was studied using a novel combination of X-ray absorption spectroscopy (XAS) at Ir L3-edge, Cl K-edge, and K K-edge. These culminate in *in situ* XAS experiments that link structural changes of the Ir complex with its catalytic activity and its deactivation. Mercury poisoning and "hot filtration" experiments ruled out leached Ir as the active catalyst. Spectroscopic evidence indicates the exchange of one chloride ligand with an alkoxide to generate the active precatalyst. The exchange of the second chloride ligand, however, leads to a potassium alkoxide—iridate species as the deactivated form of this immobilized catalyst. These findings could be widely applicable to the many homogeneous transfer hydrogenation catalysts with Cp*IrCl substructure.
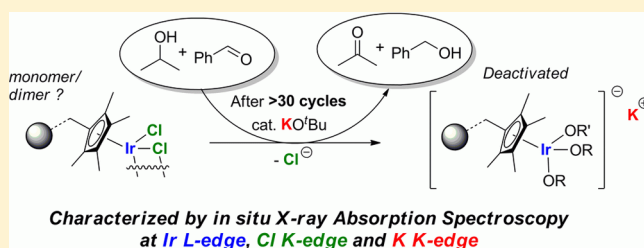
INTRODUCTION

Mechanistic understanding of the deactivation pathways, and thus possible reactivation, is vitally important in the application of catalytic reactions in industry. While many important heterogeneous catalytic processes have been studied extensively, synthetically useful catalytic reactions are often not subjected to the same level of scrutiny. Those that are well studied are invariably the most industrially important reactions: hydrogenation, hydroformylation, hydrosilylation, polymerizations, and oxidations. Common deactivation pathways in homogeneous catalysis include metal deposition, counterion inhibition, ligand exchange, and ligand consumption. These have been comprehensively reviewed by de Vries,[1] van Leeuwen and Chadwick,[2] and most recently by Crabtree.[3]

Transfer hydrogenation is an important class of catalytic reaction in chemical syntheses, particularly for chiral alcohols and amines.[4] Not only do these reactions eliminate the need for specialized hydrogenation equipment when scaled up, they also proceed with excellent selectivity under mild conditions.[4c] In addition, transfer hydrogenation forms part of the "borrowing hydrogen" mechanism, a highly atom economical and versatile concept in modern synthetic methodology.[5] Various highly

active catalysts (turnover number (TON) > 5000, turnover frequency (TOF) up to 20000 h^{-1}) have been developed (Scheme 1),[6] although their elaborated nature means catalyst recovery is important in industrial applications.[7] Numerous mechanistic studies on transfer hydrogenation by Ru/Ir half-sandwich complexes have elucidated predominantly Ru/Ir-monohydride intermediates, which react with carbonyl/imine substrates with either concerted or nonconcerted proton transfer depending on reaction conditions (Scheme 1).[6b,8] Nevertheless, insights regarding the deactivation of these catalysts, which are critical for maximizing TON, are few and often indirect.[9] In this paper, we report a mechanistic study into the deactivation of a common Cp*Ir transfer hydrogenation precatalyst.

We recently reported an immobilized transfer hydrogenation precatalyst $[Cp**IrCl_2]_2$, (Cp** = immobilized Cp* ligand) on a Wang resin support, which was reused up to 35 times in the presence of KO^{t}Bu, which will become important in the catalyst deactivation that follows (Scheme 2), using ^{i}PrOH as

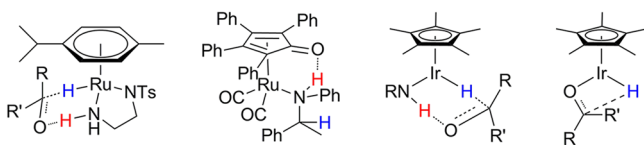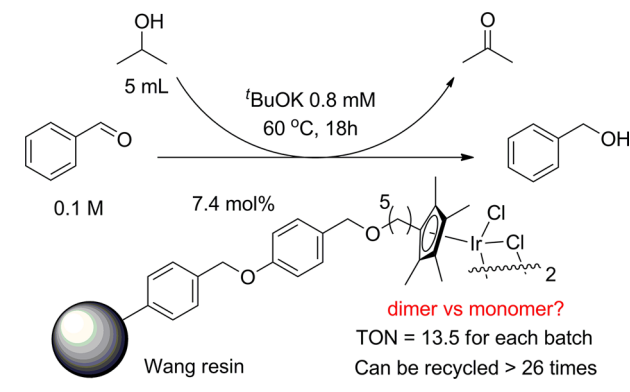**Scheme 1. Typical Ru/Ir Half-Sandwich Catalysts and Transition States in Transfer Hydrogenation[6]**
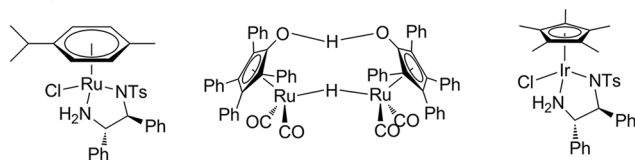
Scheme 2. Catalytic Transfer Hydrogenation Using Immobilized [Cp**IrCl_2] as Precatalyst in Batch[10]**

the hydrogen source.[10] This was achieved through a novel immobilization strategy, which links the precatalyst to the support through the η^5-Cp* ligand. A slow and partial deactivation of the catalyst was observed over 26 uses (total TON > 350). Treatment of the deactivated catalyst with dilute aqueous HCl 1 M in batch mode was found to be effective in restoring catalytic activity. This "reactivated" catalyst, however, quickly lost its activity after another three uses. While catalytic activity of $[Cp^*IrCl_2]_2$ in transfer hydrogenation is inferior to the best catalysts in the literature and was further reduced by immobilization, this catalytic system presents an excellent opportunity to study catalyst deactivation without interference from metal leaching.

X-ray absorption spectroscopy (XAS) is one of the few analytical tools that can provide structural information for immobilized homogeneous catalysts, that is, coordination number, bond lengths, and oxidation state of the element of interest.[11] XAS has been previously employed to study immobilized homogeneous catalysts,[12] including multiedge studies.[13] Nevertheless, the only studies that employed both hard and soft X-ray in the literature have been on Fe–S enzymes,[14] a Cp*Ru anticancer complex,[15] and lanthanide $[MCl_6]^{3-}$ complexes.[16] This is probably due to the technical challenges associated with in situ studies at soft X-ray energy range. We envisaged, however, that such an approach, that is, XAS at both the Ir L-edge and Cl K-edge, will provide a more complete mechanistic picture of the changes in the catalyst, given the multiphasic nature of the catalytic system, that is, solution, polymeric support, and catalyst. Such a study into the

deactivation of immobilized $[Cp^{**}IrCl_2]_2$ precatalyst in transfer hydrogenation is reported herein.

■ EXPERIMENTAL SECTION

All glassware was dried in the oven (120 °C) overnight prior to use. The XAS flow-cell was assembled and flushed with nitrogen for 30 min before experiments. Anhydrous ^iPrOH (<50 ppm water) was obtained from Sigma-Aldrich and used without further purification.

Solid state XAS measurements of various immobilized iridium precatalysts and standards at the Ir L-edge were acquired on beamline B18 at Diamond Light Source using a Si(111) monochromator at 3 GeV and 300 mA. Samples were prepared as 8 mm cellulose pellets (80 mg of cellulose) with 10 mg of the immobilized precatalyst samples or 5 mg for the iridium complexes. Transmission signal was recorded using an ionization chamber and intensity monitoring.

Ex situ Cl and K K-edge XAS measurements were performed on beamline BM28 of the European Synchrotron Radiation Facility using a Si(111) double crystal monochromator at 6 GeV and 200 mA. Cl K-edge and K K-edge spectra were collected in fluorescence mode using solid sample mounted on carbon tape under vacuum. Data analysis was performed using the software package IFEFFIT.[17]

Kinetic modeling was performed using the DynaFit package from BioKin.[18]

Typical Batch Reaction. To the immobilized precatalyst $[Cp^{**}IrCl_2]_2$ (0.057 g, 0.035 mmol Ir) in a vial was added KO^{t}Bu (0.50 mg, 0.004 mmol) and anhydrous ^iPrOH (5 mL). The mixture was stirred at 60 °C for 1 h to allow catalyst activation. Benzaldehyde (0.05 mL, 0.5 mmol) was then added. The mixture was stirred at 60 °C, and the reaction was monitored by GC. Further runs were conducted by decanting the solution and recharging the resin with KO^{t}Bu (0.5 mg, 0.004 mmol), ^iPrOH (5 mL), and benzaldehyde (0.05 mL, 0.5 mmol) immediately.

"Reactivation" of Deactivated Catalyst. The deactivated catalyst from a typical batch reaction after filtration was stirred with aqueous HCl 1 M (10 mL) at room temperature for 30 min. The catalyst was filtered, and washed with water (10 mL) and methanol (10 mL) before drying to give the "reactivated" catalyst.

In Situ XAS Experiment in Continuous Flow Cell. The reaction solution was pumped as a thin film (<100 μm) at 10.8 μL·min^{-1} over the immobilized catalyst, $[Cp^{**}IrCl_2]_2$ (1.0 mg), in a spectroscopic flow cell at 60 °C using a milliGAT positive displacement pump and 1/8 in. PTFE tubing. A schematic of the experiment setup is shown in Figure 5. At first, the catalyst was activated with a solution of KO^{t}Bu (0.89 mM) in ^iPrOH for 30 min, before being exposed to the reaction mixture containing benzaldehyde (0.10 M) and KO^{t}Bu (0.89 mM) in ^iPrOH. Catalytic conversion was monitored by GC with 1,1'-biphenyl as internal standard. More details of the experiment can be found in the Supporting Information, section 9.

■ RESULTS AND DISCUSSION

Preliminary Studies. Mechanistic insights of immobilized homogeneous catalysts are normally difficult to obtain due to the limitations of traditional analytical techniques for immobilized homogeneous catalysts. Inductive coupling plasma analysis of the iridium content of the immobilized species after 35 uses indicated only 3% decrease in Ir content, which showed little catalytic consequence based on the experiments described below.[10] A batch reaction that was poisoned with mercury (300 equiv) after 3 h showed no significant decrease in catalytic activity (see Figure S1, Supporting Information). Furthermore, a "hot filtration" experiment, wherein half of the reaction mixture was filtered and the other half was left unaltered, after 3 h demonstrated that the reaction was stopped after being filtered through a 0.2 μm syringe filter (Figure 1). These results rule out the possibility of a very small amount of leached Ir nanoparticles in solution being responsible for all the catalytic activity.[19]
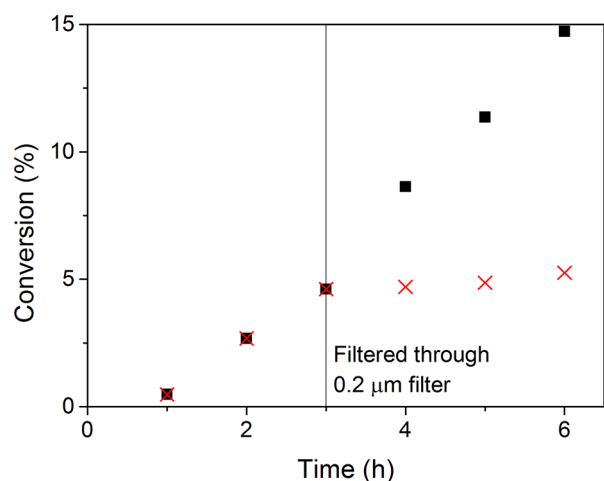
Figure 1. Catalytic conversion, determined by GC, following "hot filtration" of the reaction mixture through a 0.2 μm filter (×) and of the same reaction without "hot filtration" (■) using precatalyst $[Cp^{**}IrCl_2]_2$.

Consequently, deactivation must be associated with changes in the coordination sphere of the immobilized Ir catalyst. Previous studies suggested that the presence of a small amount of water can have a significant effect on catalytic performance and mechanism.[6b,8c,g] Accumulation of such effect over 26 cycles may explain the slow decrease in catalytic activity. An experiment to evaluate the effect of water, however, showed little difference between reaction profiles in the presence and absence of added water (5 equiv to Ir) (Figure 2).
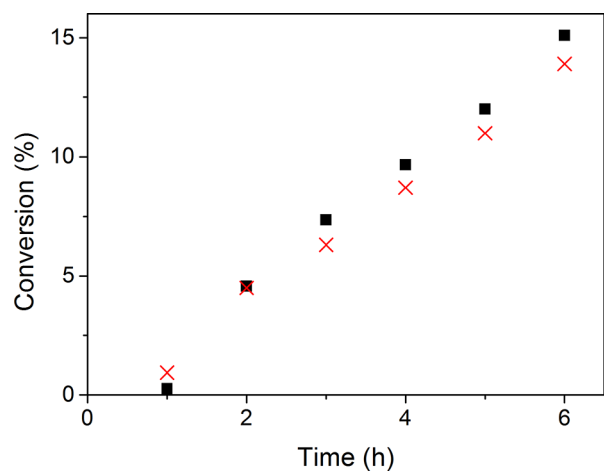

Figure 2. Catalytic conversion, determined by GC, vs time for batch reation using precatalyst $[Cp^{**}IrCl_2]_2$ under anhydrous conditions (■) and in the presence of 5 equiv (to Ir) of added water (×) as determined by GC.

***Ex Situ* XAS Study of Catalyst Deactivation.** Static samples of the fresh precatalyst, the catalyst after three uses, the deactivated catalyst (after 30 uses) and a "reactivated" catalyst were first studied using Ir L-edge extended X-ray absorption fine structure spectroscopy (EXAFS; 11.2 keV, transmission mode) and Cl K-edge X-ray absorption near edge structure spectroscopy (XANES; 2.8 keV, fluorescence mode).

The Ir L-edge EXAFS spectra of the catalysts were compared with those of $[Cp^*Ir(\mu^2\text{-}Cl)_3IrCp^*]OTf$ (**1**), $[Cp^*IrCl_2]_2$ (**2**), and $[Cp^*IrCl_2((Py))]$ (**3**) (Py = pyridine) as standards. All

Fourier-transformed spectra displayed a common pattern in radial distribution plots (Figure 3a,b), with one peak representing the Ir—C and Ir—N interactions ($R \approx 1.7$ Å) and another peak representing the longer Ir—Cl bonds ($R \approx 2.2$ Å). The relative intensity of these two peaks correlates well with the number of chloride ligands on the Ir catalyst (Figure 3c). Importantly, the fresh catalyst showed a similar ratio between the intensities of Ir—C and Ir—Cl signals compared with those of $[Cp^*IrCl_2(Py)]$ (Figure 3c). This suggests that there are two chloride ligands on each Ir cation on average in the fresh precatalyst, In other words, the immobilized precatalyst exists in a monomeric $[Cp^{**}IrCl_2(S)]$ (S = neutral ligand) rather than its dimeric form $[Cp^{**}IrCl_2]_2$, in which each Ir cation has three chloride ligands in its coordination sphere before immobilization.

Comparing the spectra of the immobilized catalysts at various stages showed rapid partial loss of chloride ligands (~50%) after 3 uses (Figure 3b), despite little decrease in catalytic activity,[10] indicating only one chloride ligand in the activated precatalyst. After 30 uses, no Ir—Cl signal was observed in the EXAFS spectrum. Furthermore, treatment with aqueous HCl 1 M to give the 'reactivated' catalyst did not reintroduce the chloride ligands, as indicated by a complete lack of Ir—Cl signal in the Ir K-edge EXAFS spectrum of this species (Figure 3b). This agrees with the rapid loss of catalytic activity in this "reactivated" catalyst after 3 uses.

The decrease in Ir—Cl signals above was corroborated by Cl K-edge XANES spectra where corresponding decreases in the edge jump, that is, absorption according to Lambert—Beer law, in the samples after 3 and 30 uses were observed. These suggest that the chloride anions were lost to the reaction solution and were no longer associated with the immobilized precatalyst (Figure 3d). However, normalized spectra, that is, scaled spectra that remove signal strength difference due to concentration, suggested little change in the coordination environment of the remaining chloride after 3 and 30 uses. To our surprise, the "reactivation" with aqueous HCl 1 M did increase the chlorine content despite the lack of an Ir—Cl signal in Ir L-edge EXAFS spectrum (Figure 3c). However, the Cl K-edge XANES spectrum of this sample is significantly different from those of others, indicating a new form of chlorine. This new species was deduced to be KCl (from the KO^{t}Bu in the batch reaction), and its identity was confirmed by comparison to the Cl K-edge XANES spectrum of the authentic KCl salt (Figure 4). Two possible explanations for this formation of KCl could be proposed: (i) by reaction of HCl with small amount of KO^{t}Bu trapped in the support or (ii) by reaction of HCl with the deactivated catalyst, which contains potassium cation.

***In Situ* XAS Study of Catalyst Deactivation.** An *in situ* experiment was performed to directly link catalyst deactivation and the loss of chloride ligands (Figure 5a), using a flow-cell to house a fixed bed of the precatalyst (see section 11, Supporting Information). The reaction solution was flowed over the catalyst as a thin film (<100 μm) at 60 °C for 24 h. Fluorescence XANES spectra at Cl and K K-edge (2.8 and 3.6 keV, respectively) were collected to monitor the changes of the immobilized catalyst. The solution from the flow-cell was collected (without X-ray radiation) and analyzed using gas chromatography (GC) to evaluate the activity of the catalyst bed.

Catalyst activation in the batch protocol was replicated by flowing a solution of KO^{t}Bu through the flow cell for 30 min.[10] A corresponding ~50% decrease in chlorine content was

(a)

(b)

(c)

(d)

Figure 4. Normalized XANES spectra of KCl (red solid line) and the "reactivated" catalyst (black dashed line).

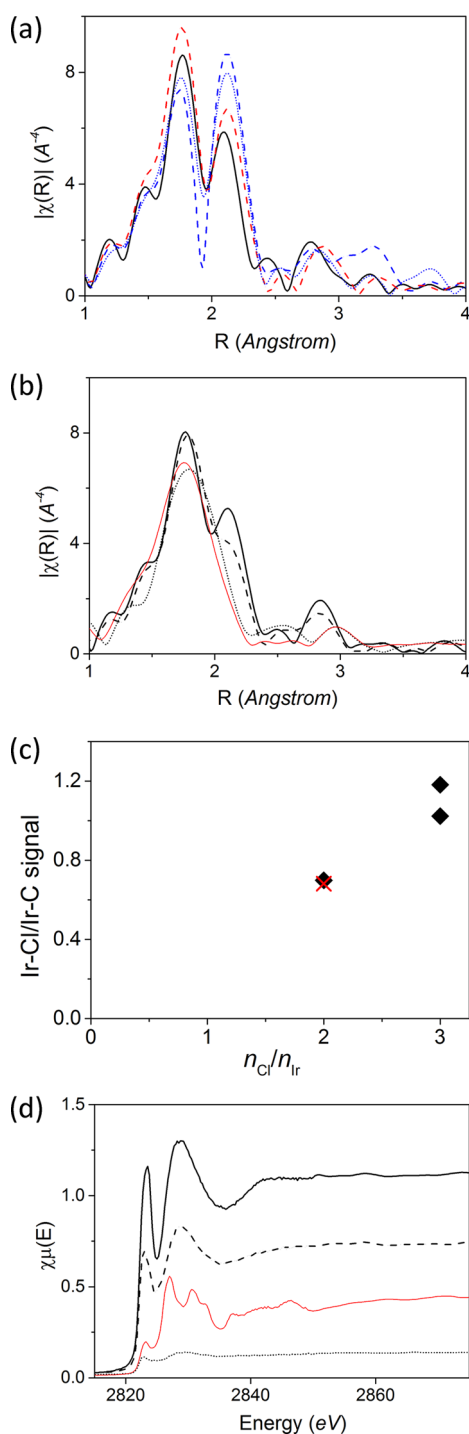**Figure 3.** XAS results of *ex situ* samples and standards: (a) Fourier-transformed Ir L-edge EXAFS spectra of standards **1** (blue dashed line), **2** (blue dotted line), and **3** (red dashed line) and the fresh precatalyst (black solid line); (b) Fourier-transformed Ir L-edge EXAFS spectra of various stages of the immobilized catalyst, fresh precatalyst (black solid line), catalyst after three uses (black dashed line), catalyst after 30 uses (blue dotted line), and "reactivated" catalyst (red solid line); (c) signal ratio of Ir−Cl/Ir−C vs number of Cl coordinated to each Ir in standards **1**, **2**, and **3** (◆) and fresh precatalyst (✕); (d) Cl K-edge XANES spectra of the fresh precatalyst (black solid line), catalyst after three uses (black dashed line), catalyst after 30 uses (blue dotted line), and "reactivated" catalyst (red solid line).
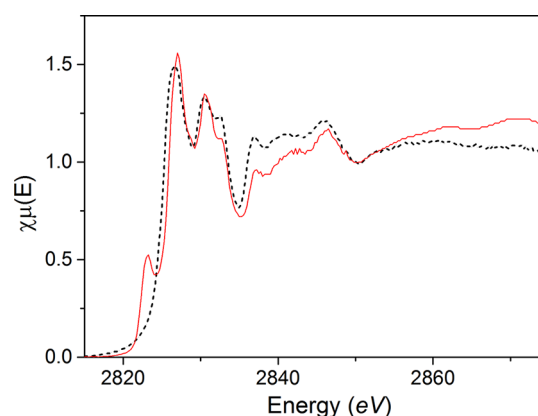
observed, with a small increase in potassium content (Figure 5b). This change is consistent with the replacement of one chloride ligand with an alkoxide (O^{i}Pr or O^{t}Bu) to generate complex [Cp**IrCl(OR)(S)] (R = ^{i}Pr or ^{t}Bu, S = neutral ligand), which is the dominant species before catalytic turnover. This observation is also in agreement with the spectra of *ex situ* samples above (Figure 3b) wherein a rapid loss of the first chloride ligand did not result in deactivation. This is the first spectroscopic evidence of such species under catalytically relevant conditions,[20] although similar complexes has been previously synthesized with S = PAr$_3$,[21] and N-pyridine/ quinoline derivatives,[22] A more recent example is a Cp*Ir catalyst for oxidation of water and C−H activation reported by Crabtree and co-workers.[23]

The reaction solution was then flowed through the cell at 60 °C. A gradual decrease in the chlorine content was observed with a corresponding increase in the potassium content (Figure 5c). The systematic error of the measurement was larger with chlorine than with potassium, due to both the lower energy of Cl K-edge and the diminishing amount of chlorine over time. Importantly, decreasing conversion of benzaldehyde to benzyl alcohol by the catalyst was observed on the same time scale (Figure 6).

The two-step behavior of this plot could be attributed to the heterogeneous nature of the catalyst. A simple fitting for catalytic activity over time with first order deactivation processes confirmed its two-step nature (see section 14, Supporting Information). A fast deactivation and a slow deactivation are required to achieve a good fit with experimental data. Kinetics of immobilized catalysts is often further complicated by limited mass transfer and physical/ chemical changes to the support, which are difficult to quantify.[24] However, initial deactivation of catalytic centers on the surface of the polymer support should have a much more pronounced effect on the observed catalytic activity than deactivation of catalytic centers deep inside the support matrix. While acceleration effect of X-ray radiation on chemical reaction due to local heating effect is known,[25] the similar time scales of the changes in the structure of the catalyst and catalytic activity were reassuring. The steady build up in potassium content, which was not removed by washing with ^{i}PrOH, indicates that potassium cation forms an integral part of the deactivated catalyst, rather than simply being trapped in the polymer support.
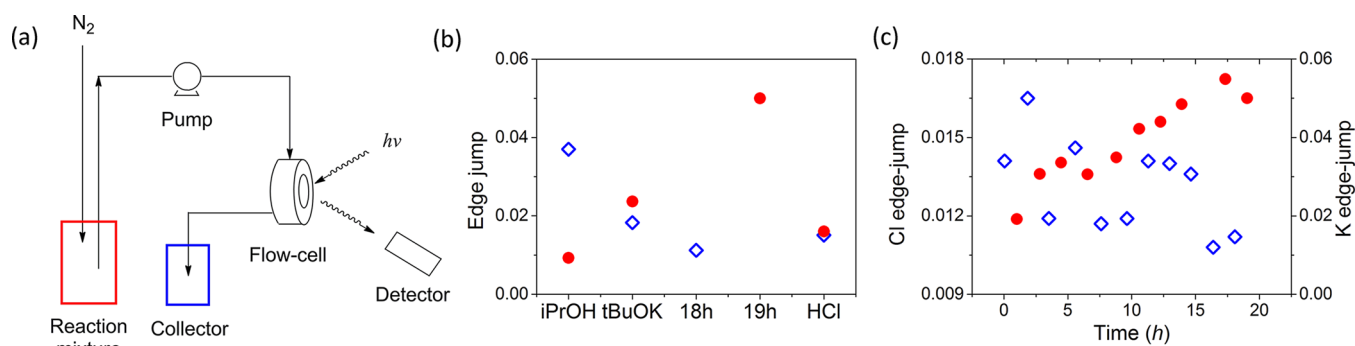
Figure 5. *In situ* XAS experiment at Cl K-edge and K K-edge: (a) experimental setup for *in situ* fluorescence XANES; (b) Cl K-edge jump (◇) and K K-edge jump (●) after activation and "reactivation"; (c) Cl K-edge jump (◇) and K K-edge jump (●) under turnover conditions.

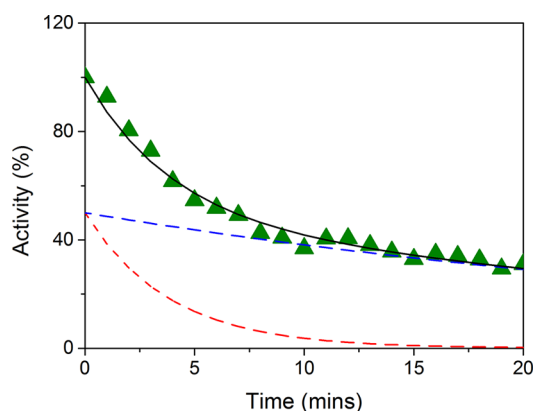**Figure 6.** Loss of catalytic activity (▲) over 20 h compared with that of fresh precatalyst by GC and a kinetic fitting of catalyst deactivation process with two deactivation processes: fast (red dashed line) and slow (blue dashed line).

Scheme 3. Proposed Deactivation and "Reactivation" Pathways

A pulse of aqueous HCl 1 M was pumped through the catalyst bed to mimic the temporary "reactivation" of the catalyst. This was followed by washing with ^{i}PrOH. As expected from the spectra of static samples, no increase in chlorine content was observed. However, KCl was not detected in the immobilized catalyst because it was washed out by ^{i}PrOH (Figure 5b). This suggests that the hypothesis that the potassium cation was structurally part of the deactivated catalyst is the more likely scenario. Both KCl and KO^{t}Bu were easily removed from the support matrix of the immobilized catalyst with sufficient ^{i}PrOH washing in our flow cell.

The various spectroscopic results at Ir L-edge, Cl K-edge, and K K-edge clearly suggest an anionic Ir complex with a potassium counterion as the deactivated form of the catalyst. This species is formed as the catalyst exchanges its last chloride ligand with alkoxide to give a potassium iridate complex (Scheme 3).[26] Although trialkoxide-Cp*-iridates are not known in the literature, examples have been reported for azomethineylides, halides,[27] and cyanide.[28] Most of the proposed mechanisms for this type of transfer hydrogenation require two coordination sites (Scheme 1), for the hydride and the ketone/aldehyde[8i] or for the alcohol and the ketone/aldehyde in a Meerwein−Ponndorf−Verley mechanism.[29] Consequently, the steric hindrance around Ir due to the alkoxide ligands (^{t}BuO or ^{i}PrO) and the strength of the Ir−alkoxide bonds are likely to be responsible for the decrease in catalytic activity.

The proposed deactivated catalyst also explains the temporary reactivation by treatment with aqueous 1 M HCl.
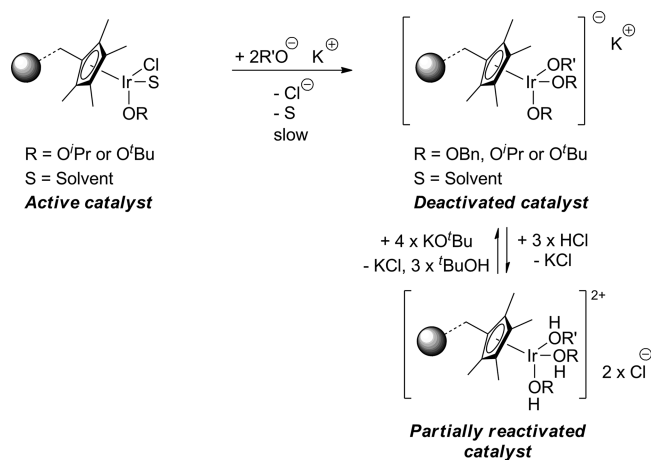
This protocol leads to protonation of the alkoxide ligands, making them more labile and readily replaced by benzaldehyde to allow catalytic turnover. This is consistent with the reported activity of Cp*Ir species, for example, [Cp*Ir(OH$_2$)$_3$]SO$_4$ and [Cp*Ir(NH$_3$)$_3$]X (X = Cl, I), which have been shown to readily exchange ligands and form active catalysts in transfer hydrogenation.[26,30]

A comparison of the active catalyst vs the proposed partially active catalyst suggests that other methods of reactivation may be successful and that prediction is currently being evaluated by *in situ* XAS and other studies.

■ **CONCLUSION**

In summary, we report the first study of an immobilized homogeneous transfer hydrogenation precatalyst using XAS at both hard and soft X-ray for Ir, Cl, and K. This novel combination of techniques allowed us to probe and understand the catalyst deactivation in detail. Such insight could not have been achieved with any other technique currently available to chemists or with single element XAS. Furthermore, the relevance of the deactivation pathway, through ligand exchange with alkoxides, is applicable to many homogeneous catalysts for transfer hydrogenation with similar Cp*IrCl structural motifs. Studies to more effectively reactivate the immobilized catalyst, that is, reintroducing a chloride ligand on iridium, are in progress and will be disseminated in due course.

■ ASSOCIATED CONTENT

Ⓢ Supporting Information

Experimental details and characterization data. This material is available free of charge via the Internet at http://pubs.acs.org.

■ AUTHOR INFORMATION

Corresponding Author

*b.nguyen@leeds.ac.uk

Notes

The authors declare no competing financial interest.

■ ACKNOWLEDGMENTS

■ REFERENCES

(1) Heller, D.; de Vries, A. H. M.; de Vries, J. G. Catalyst Inhibition and Deactivation in Homogeneous Hydrogenation. In *The Handbook of Homogeneous Hydrogenation*; de Vries, J. G., Elsevier, C. J., Eds.; Wiley-VCH Verlag GmbH & Co. KGaA: Weinheim, Germany, 2007; pp 1483−1516.

(2) (a) Castarlenas, R. *Catal. Lett.* **2013**, *143*, 748−748. (b) van Leeuwen, P. W. N. M. *Appl. Catal., A* **2001**, *212*, 61−81.

(3) (a) Crabtree, R. H. *Chem. Rev.* **2015**, *115*, 127−150. (b) Crabtree, R. H. *J. Organomet. Chem.* **2014**, *751*, 174−180.

(4) (a) Sues, P. E.; Demmans, K. Z.; Morris, R. H. *Dalton Trans.* **2014**, *43*, 7650−7667. (b) Morris, R. H. *Chem. Soc. Rev.* **2009**, *38*, 2282−2291. (c) Ikariya, T.; Blacker, A. J. *Acc. Chem. Res.* **2007**, *40*, 1300−1308. (d) Gladiali, S.; Alberico, E. *Chem. Soc. Rev.* **2006**, *35*, 226−236.

(5) (a) Nixon, T. D.; Whittlesey, M. K.; Williams, J. M. J. *Dalton Trans.* **2009**, 753−762. (b) Hamid, M. H. S. A.; Slatford, P. A.; Williams, J. M. J. *Adv. Synth. Catal.* **2007**, *349*, 1555−1575.

(6) (a) Cotarca, L.; Verzini, M.; Volpicelli, R. *Chim. Oggi* **2014**, *32*, 36−41. (b) Wu, X.; Liu, J.; Di Tommaso, D.; Iggo, J. A.; Catlow, C. R. A.; Bacsa, J.; Xiao, J. *Chem.—Eur. J.* **2008**, *14*, 7699−7715. (c) Karvembu, R.; Prabhakaran, R.; Natarajan, K. *Coord. Chem. Rev.* **2005**, *249*, 911−918. (d) Shvo, Y.; Czarkie, D.; Rahamim, Y.; Chodosh, D. F. *J. Am. Chem. Soc.* **1986**, *108*, 7400−7402.

(7) (a) Ito, J.-I.; Nishiyama, H. *Tetrahedron Lett.* **2014**, *55*, 3133−3146. (b) Štefane, B.; Požgan, F. *Catal. Rev.* **2014**, *56*, 82−174. (c) Darwish, M.; Wills, M. *Catal. Sci. Technol.* **2012**, *2*, 243−255. (d) Fleury-Brégeot, N.; de la Fuente, V.; Castillón, S.; Claver, C. *ChemCatChem* **2010**, *2*, 1346−1371.

(8) (a) Campos, J.; Hintermair, U.; Brewster, T. P.; Takase, M. K.; Crabtree, R. H. *ACS Catal.* **2014**, *4*, 973−985. (b) Kuzma, M.; Vaclavik, J.; Novak, P.; Prech, J.; Januscak, J.; Cerveny, J.; Pechacek, J.; Sot, P.; Vilhanova, B.; Matousek, V.; Goncharova, I. I.; Urbanova, M.; Kacer, P. *Dalton Trans.* **2013**, *42*, 5174−5182. (c) Pavlova, A.; Meijer, E. J. *ChemPhysChem* **2012**, *13*, 3492−3496. (d) Guo, X.; Tang, Y.; Zhang, X.; Lei, M. *J. Phys. Chem. A* **2011**, *115*, 12321−12330. (e) Pannetier, N.; Sortais, J.-B.; Dieng, P. S.; Barloy, L.; Sirlin, C.; Pfeffer, M. *Organometallics* **2008**, *27*, 5852−5859. (f) Handgraaf, J.-W.; Meijer, E. J. *J. Am. Chem. Soc.* **2007**, *129*, 3099−3103. (g) Samec, J. S. M.; Ell, A. H.; Aaberg, J. B.; Privalov, T.; Eriksson, L.; Baeckvall, J.-E. *J. Am. Chem. Soc.* **2006**, *128*, 14293−14305. (h) Sandoval, C. A.; Ohkuma, T.; Utsumi, N.; Tsutsumi, K.; Murata, K.; Noyori, R. *Chem.—Asian J.* **2006**, *1*, 102−110. (i) Samec, J. S. M.; Backvall, J.-E.; Andersson, P. G.; Brandt, P. *Chem. Soc. Rev.* **2006**, *35*, 237−248. (j) Casey, C. P.; Johnson, J. B. *J. Org. Chem.* **2003**, *68*, 1998−2001. (k) Sandoval, C. A.; Ohkuma, T.; Muniz, K.; Noyori, R. *J. Am. Chem. Soc.* **2003**, *125*, 13490−13503. (l) Yi, C. S.; He, Z.; Guzei, I. A. *Organometallics* **2001**, *20*, 3641−3643. (m) Yamakawa, M.; Ito, H.; Noyori, R. *J. Am. Chem. Soc.* **2000**, *122*, 1466−1478. (n) Haack, K.-J.;

Hashiguchi, S.; Fujii, A.; Ikariya, T.; Noyori, R. *Angew. Chem., Int. Ed.* **1997**, *36*, 285−288. (o) Hashiguchi, S.; Fujii, A.; Takehara, J.; Ikariya, T.; Noyori, R. *J. Am. Chem. Soc.* **1995**, *117*, 7562−7563.

(9) (a) Lagaditis, P. O.; Sues, P. E.; Lough, A. J.; Morris, R. H. *Dalton Trans.* **2015**, DOI: 10.1039/C4DT02799J. (b) Liu, C.; Liao, S.; Li, Q.; Feng, S.; Sun, Q.; Yu, X.; Xu, Q. *J. Org. Chem.* **2011**, *76*, 5759−5773. (c) Sun, X.; Manos, G.; Blacker, J.; Martin, J.; Gavriilidis, A. *Org. Process Res. Dev.* **2004**, *8*, 909−914. (d) Everaere, K.; Mortreux, A.; Bulliard, M.; Brussee, J.; Van der Gen, A.; Nowogrocki, G.; Carpentier, J.-F. *Eur. J. Org. Chem.* **2001**, 275−291.

(10) Lucas, S. J.; Crossley, B. D.; Pettman, A. J.; Vassileiou, A. D.; Screen, T. E. O.; Blacker, A. J.; McGowan, P. C. *Chem. Commun.* **2013**, *49*, 5562−5564.

(11) (a) Garino, C.; Borfecchia, E.; Gobetto, R.; van Bokhoven, J. A.; Lamberti, C. *Coord. Chem. Rev.* **2014**, *277−278*, 130−186. (b) Bunker, G. *Introduction to XAFS: A Practical Guide to X-ray Absorption Fine Structure Spectroscopy*; Cambridge University Press: Cambridge, U.K., 2010.

(12) (a) Brazier, J. B.; Nguyen, B. N.; Adrio, L. A.; Barreiro, E. M.; Leong, W. P.; Newton, M. A.; Figueroa, S. J. A.; Hellgardt, K.; Hii, K. K. M. *Catal. Today* **2014**, *229*, 95−103. (b) Choe, J. K.; Boyanov, M. I.; Liu, J.; Kemner, K. M.; Werth, C. J.; Strathmann, T. J. *J. Phys. Chem. C* **2014**, *118*, 11666−11676. (c) Colomban, C.; Kudrik, E. V.; Afanasiev, P.; Sorokin, A. B. *J. Am. Chem. Soc.* **2014**, *136*, 11321−11330. (d) Kraft, S. J.; Hu, B.; Zhang, G.; Miller, J. T.; Hock, A. S. *Eur. J. Inorg. Chem.* **2013**, *2013*, 3972−3977. (e) Schoenfeldt, N. J.; Ni, Z.; Korinda, A. W.; Meyer, R. J.; Notestein, J. M. *J. Am. Chem. Soc.* **2011**, *133*, 18684−18695.

(13) (a) Greco, G.; Witkowska, A.; Minicucci, M.; Olivi, L.; Principi, E.; Dsoke, S.; Moretti, A.; Marassi, R.; Di Cicco, A. *J. Phys. Chem. C* **2012**, *116*, 12791−12802. (b) Velu, S.; Suzuki, K.; Gopinath, C. S.; Yoshida, H.; Hattori, T. *Phys. Chem. Chem. Phys.* **2002**, *4*, 1990−1999. (c) Fiddy, S. G.; Newton, M. A.; Campbell, T.; Corker, J. M.; Dent, A. J.; Harvey, I.; Salvini, G.; Turin, S.; Evans, J. *Chem. Commun.* **2001**, 445−446. (d) Murphy, L. M.; Strange, R. W.; Hasnain, S. S. *Structure* **1997**, *5*, 371−379. (e) Sadoc, A.; Lagarde, P.; Vlaic, G. *J. Phys. C* **1985**, *18*, 23.

(14) (a) Silver, S.; Gardenghi, D.; Naik, S.; Shepard, E.; Huynh, B.; Szilagyi, R.; Broderick, J. *J. Biol. Inorg. Chem.* **2014**, *19*, 465−483. (b) Giles, L. J.; Grigoropoulos, A.; Szilagyi, R. K. *J. Phys. Chem. A* **2012**, *116*, 12280−12298.

(15) Sriskandakumar, T.; Petzold, H.; Bruijnincx, P. C. A.; Habtemariam, A.; Sadler, P. J.; Kennepohl, P. *J. Am. Chem. Soc.* **2009**, *131*, 13355−13361.

(16) Löble, M. W.; Keith, J. M.; Altman, A. B.; Stieber, S. C. E.; Batista, E. R.; Boland, K. S.; Conradson, S. D.; Clark, D. L.; Lezama Pacheco, J.; Kozimor, S. A.; Martin, R. L.; Minasian, S. G.; Olson, A. C.; Scott, B. L.; Shuh, D. K.; Tyliszczak, T.; Wilkerson, M. P.; Zehnder, R. A. *J. Am. Chem. Soc.* **2015**, *137*, 2506−2523.

(17) Newville, M. *J. Synchrotron Radiat.* **2001**, *8*, 322−324.

(18) Kuzmič, P. *Anal. Biochem.* **1996**, *237*, 260−273.

(19) (a) Bayram, E.; Linehan, J. C.; Fulton, J. L.; Roberts, J. A. S.; Szymczak, N. K.; Smurthwaite, T. D.; Özkar, S.; Balasubramanian, M.; Finke, R. G. *J. Am. Chem. Soc.* **2011**, *133*, 18889−18902. (b) Widegren, J. A.; Finke, R. G. *J. Mol. Catal. A: Chem.* **2003**, *198*, 317−341.

(20) Attempts to prepare such complex with from non-immobilized [Cp*IrCl2]2 have all been unsuccessful due to decomposition of the products.

(21) Yamamoto, Y.; Sugawara, K.; Kakeya, M. *Inorg. Chim. Acta* **2002**, *340*, 21−28.

(22) (a) Thai, T.-T.; Therrien, B.; Suss-Fink, G. *Inorg. Chem. Commun.* **2009**, *12*, 806−807. (b) Fujita, K.-i.; Tanino, N.; Yamaguchi, R. *Org. Lett.* **2006**, *9*, 109−111. (c) Yamamoto, Y.; Kawasaki, K.; Nishimura, S. *J. Organomet. Chem.* **1999**, *587*, 49−57.

(23) (a) Zhou, M.; Hintermair, U.; Hashiguchi, B. G.; Parent, A. R.; Hashmi, S. M.; Elimelech, M.; Periana, R. A.; Brudvig, G. W.; Crabtree, R. H. *Organometallics* **2013**, *32*, 957−965. (b) Parent, A. R.; Brewster, T. P.; De Wolf, W.; Crabtree, R. H.; Brudvig, G. W. *Inorg. Chem.* **2012**, *51*, 6147−6152. (c) Zhou, M.; Balcells, D.; Parent, A. R.; Crabtree, R.

H.; Eisenstein, O. *ACS Catal.* **2012**, *2*, 208−218. (d) Schley, N. D.; Blakemore, J. D.; Subbaiyan, N. K.; Incarvito, C. D.; D'Souza, F.; Crabtree, R. H.; Brudvig, G. W. *J. Am. Chem. Soc.* **2011**, *133*, 10473−10481.

(24) Tóth, I.; Van Geem, P. C., Immobilization Techniques. In *The Handbook of Homogeneous Hydrogenation*; Wiley-VCH Verlag GmbH: 2006; pp 1421−1467.

(25) Guilera, G.; Newton, M. A.; Polli, C.; Pascarelli, S.; Guino, M.; Hii, K. K. *Chem. Commun.* **2006**, 4306−4308.

(26) Wöckel, S.; Plessow, P.; Schelwies, M.; Brinks, M. K.; Rominger, F.; Hofmann, P.; Limbach, M. *ACS Catal.* **2013**, *4*, 152−161.

(27) Song, G.; Chen, D.; Su, Y.; Han, K.; Pan, C.-L.; Jia, A.; Li, X. *Angew. Chem., Int. Ed.* **2011**, *50*, 7791−7796.

(28) M. Contakes, S.; Schmidt, M.; B. Rauchfuss, T. *Chem. Commun.* **1999**, 1183−1184.

(29) (a) Handgraaf, J.-W.; Reek, J. N. H.; Meijer, E. J. *Organometallics* **2003**, *22*, 3150−3157. (b) Trocha-Grimshaw, J.; Henbest, H. B. *Chem. Commun.* **1967**, 544−544. (c) Verley, A. *Bull. Soc. Chim. Fr.* **1925**, *37*, 537. (d) Meerwein, H.; Schmidt, R. *Liebigs Ann.* **1925**, *444*, 221−238.

(30) (a) Zerla, D.; Facchetti, G.; Fusè, M.; Pellizzoni, M.; Castellano, C.; Cesarotti, E.; Gandolfi, R.; Rimoldi, I. *Tetrahedron: Asymmetry* **2014**, *25*, 1031−1037. (b) Vázquez-Villa, H.; Reber, S.; Ariger, M. A.; Carreira, E. M. *Angew. Chem., Int. Ed.* **2011**, *50*, 8979−8981. (c) Poth, T.; Paulus, H.; Elias, H.; Dücker-Benfer, C.; van Eldik, R. *Eur. J. Inorg. Chem.* **2001**, 1361−1369.